Podo, F., & Blasie, J. K. (1977) *Proc. Natl. Acad. Sci. U.S.A. 74*, 1032–1036.
Scott, T. G., Spencer, R. D., Leonard, N. J., & Weber, G. (1970) *J. Am. Chem. Soc. 92*, 687–695.
Shaklai, N. Yguerabide, J., & Ranney, H. M. (1977) *Biochemistry 16*, 5585–5592.
Shinitzky, M. (1972) *J. Chem. Phys. 56*, 5979–5981.
Snyder, B., & Freire, E. (1982) *Biophys. J. 40*, 137–148.
Thulborn, K. R., & Sawyer, W. H. (1978) *Biochim. Biophys. Acta 511*, 125–140.
Vincent, M., Forest, B., Gallay, J., & Alfsen, A. (1982) *Biochemistry 21*, 708–716.

High-Resolution Cross-Polarization/Magic Angle Spinning ^{13}C NMR of Intracytoplasmic Membrane and Light-Harvesting Bacteriochlorophyll–Protein of Photosynthetic Bacteria†

Tsunenori Nozawa,* Mitsushi Nishimura, and Masahiro Hatano
Chemical Research Institute of Non-aqueous Solutions, Tohoku University, Sendai 980, Japan
Hidenori Hayashi
Department of Chemistry, Faculty of Science, The University of Tokyo, Bunkyo-ku, Tokyo 113, Japan
Keizo Shimada
Department of Biology, Faculty of Science, Tokyo Metropolitan University, Fukazawa, Setagaya-ku, Tokyo 158, Japan
Received July 2, 1984

ABSTRACT: Solid-state ^{13}C NMR spectra of intracytoplasmic membrane (ICM) and light-harvesting bacteriochlorophyll–protein complex 2 (LH2) of *Rhodopseudomonas palustris* were observed first at 75.46 MHz (under a 7.05 T static magnetic field) by a high-power decoupling, cross-polarization and magic angle spinning (MAS) methods in conjunction with total elimination of spinning side band techniques. At the MAS rate of 3300 Hz, ICM and LH2 yielded ^{13}C NMR spectra with high resolution. The variation of contact times yields selected NMR spectra which are mostly attributed to the proteins, lipids, and bacteriochlorophyll *a*, respectively. Further, the relaxation rates for resolved resonances were determined, and the dynamic behavior of the lipid, protein, and bacteriochlorophyll *a* was discussed in terms of the estimated relaxation rates.

The photosynthetic apparatus of the photoheterotrophic bacterium *Rhodopseudomonas palustris* is localized in a system of intracytoplasmic membrane (ICM)[1] (Cohen-Bazire & Sistrom, 1966) which, upon mechanical disruption, gives rise to small membrane vesicles occasionally called "chromatophores" (Niederman & Gibson, 1978). ICM contains most of the light-harvesting (LH) and reaction center bacteriochlorophyll (BChl) *a*–protein complexes (Niederman & Gibson, 1978). Absorption spectra revealed that these LH complexes are composed of several components designated as B870, B850, and B800 on the basis of their absorption maxima in the near-infrared (Sistrom, 1964). Two types of LH–BChl–proteins have been isolated from chromatophores of *Rps. palustris*. These were designated as LH1 and LH2. LH1 is the LH–BChl–protein that includes B870, and LH2 is the one that contains B850 and B800 (Hayashi et al., 1982a–c).

Because of high molecular weights and restricted molecular motions, the BChl–proteins in solution could not give high-resolution ^{13}C NMR signals by the conventional FT NMR method for low molecular weight compounds in solutions. Hence, the use of NMR for the photosynthetic system had been limited. However, the solid-state high-resolution NMR techniques have emerged as a powerful method to obtain high-resolution ^{13}C NMR spectra of solid samples (such as ICM and BChl–proteins) which allow us to discuss dynamic structures of the photosynthetic system in situ.

In general the effects of ^{1}H–^{13}C magnetic dipole–dipole interactions, ^{13}C chemical shift anisotropies, and the time bottleneck of long ^{13}C spin–lattice relaxation times render the direct application of the liquid-state ^{13}C NMR technique to solid samples essentially useless, yielding broad and featureless spectra of low intensity. Pines et al. introduced the technique of high-power ^{1}H decoupling for eliminating the broadening effect of ^{1}H–^{13}C dipolar interactions, with ^{13}C–^{1}H cross-polarization (CP) to circumvent the ^{13}C–T_1 bottleneck (Pines et al., 1973). Schaefer & Stejskal (1976) then introduced the use of magic angle spinning (MAS) to average out the ^{13}C chemical shift anisotropy (Andrew, 1971) and demonstrated that the CP/MAS combination provides a powerful technique that is capable of yielding high-resolution ^{13}C NMR spectra of solid samples.

In this paper we will report a benefit of the application of the solid-state ^{13}C NMR (called CP/MAS NMR) to some complex biomolecular systems (ICM and LH proteins). Since the resolution was high enough to identify each carbon resonance, the dynamic structures of the constituents, i.e., protein, BChl *a*, and lipid, could be explored. Recently ^{13}C CP/MAS NMR spectra have been reported on chlorophyll *a* (Brown et

† This work was supported in part by a Grant-in-Aid for Scientific Research from the Ministry of Education, Science and Culture, Japan, and by a grant from Nissan Science Foundation to M.H.

[1] Abbreviations: CP, cross-polarization; ICM, intracytoplasmic membrane; LH, light harvesting; *Rps.*, *Rhodopseudomonas*; MAS, magic angle spinning; SDS, sodium dodecyl sulfate; NMR, nuclear magnetic resonance; Me_4Si, tetramethylsilane; TOSS, total elimination of spinning side bands; FT, Fourier transform.

0006-2960/85/0424-1890$01.50/0

al., 1984) and octaethylporphyrin (Okazaki & Mcdowell, 1984).

Materials and Methods

Materials. Rps. palustris was cultured anaerobically under continuous illumination for 4–6 days in the medium reported previously (Hayashi et al., 1982a). ICM preparation was obtained as described previously (Hayashi et al., 1982b). For preparation of LH2 it was solubilized with a mixture of sodium dodecyl sulfate (SDS) [in the final concentration of 0.8% (w/v)] and Triton X-100 [in the final concentration of 0.8% (v/v)]. The LH2 complex was separated with polyacrylamide gel electrophoresis under a buffer system containing 0.05% (w/v) SDS and 0.05% (v/v) Triton X-100 as detergents (Hayashi et al., 1982b) and further purified by the second electrophoresis and DEAE-cellulose column chromatography.

Methods. Solid-state ^{13}C CP/MAS spectra were obtained on a Bruker CXP-300 FT NMR spectrometer in conjunction with a Bruker type Z32PE/MAS probe which has an Andrew-Beans-type spinning apparatus. The spinner was made of boron nitride coated with a very thin Teflon film with an internal volume of approximately 450 μL (Ohtsuka et al., 1984) and was spun with compressed air at approximately 3.33 kHz. The adjustment of the spinning angle to the magic angle was performed to make the half-bandwidth of the carbonyl ^{13}C resonance of glycine at 176 ppm as narrow as possible (less than 30 Hz). Adamantane was utilized to match the "Hartman–Hahn" condition of $H_{1C}\gamma_C = H_{1H}\gamma_H$, where γ_C and γ_H are the magnetogyric ratios of ^1H and ^{13}C and H_{1H} and H_{1C} are the magnitudes of the respective spin locking fields, and to determine the 90° pulse of the proton (ca. 5 μs). Under these conditions the H_1 fields for ^1H and ^{13}C were 11.7 and 46.5 G (1 G = 1 × 10^{-4} T). The higher field peak of adamantane was set to 28.7 ppm, which gives the chemical shift scale relative to tetramethylsilane (Me_4Si).

Results

^{13}C CP/MAS Spectra of ICM. The solid-state ^{13}C NMR spectra of freeze-dried ICM on *Rps. palustris* were observed by the CP/MAS techniques with the varied contact times from 0.05 to 5 ms. We used also Dixon's pulse program (Dixon, 1982) which totally eliminates the spinning side bands (TOSS). Typical results are shown in Figure 1, where spinning side bands were totally eliminated and a very broad background was also taken away.

Assignments for each carbon can be made on the basis of known chemical shift assignments from solution spectra of model compounds (Bremser et al., 1978; Wüthrich, 1976). The aliphatic carbons appear from 15 to 34 ppm, and the C_α carbons of the peptide backbones of the proteins are present in the range from 43 to 65 ppm. The NMR signals from the lipid glycerol backbone exist in the region near 70 ppm. The signals around 93 and 103 ppm are due to carbons from carbohydrate (mostly glycolipids). The olefinic carbons in BChl *a* and the aromatic carbons of the protein side chains display resonances from 123 to 138 ppm. The signals around 174 ppm are attributed to the carbonyl carbons from phospholipids and the peptide backbones.

The contact time dependence of the intensities of the well-resolved resonances was plotted in Figure 2. With the increase of the contact time duration most of signals rapidly reach maxima around 0.5–1.0 ms and gradually decay. The main peaks of ^{13}C NMR signals for ICM at the contact time of 0.1 ms were assigned to resonances of peptide backbones (40–60 ppm) and side chains (15–30 ppm). On the other hand, the observation with the contact time of 5 ms displays

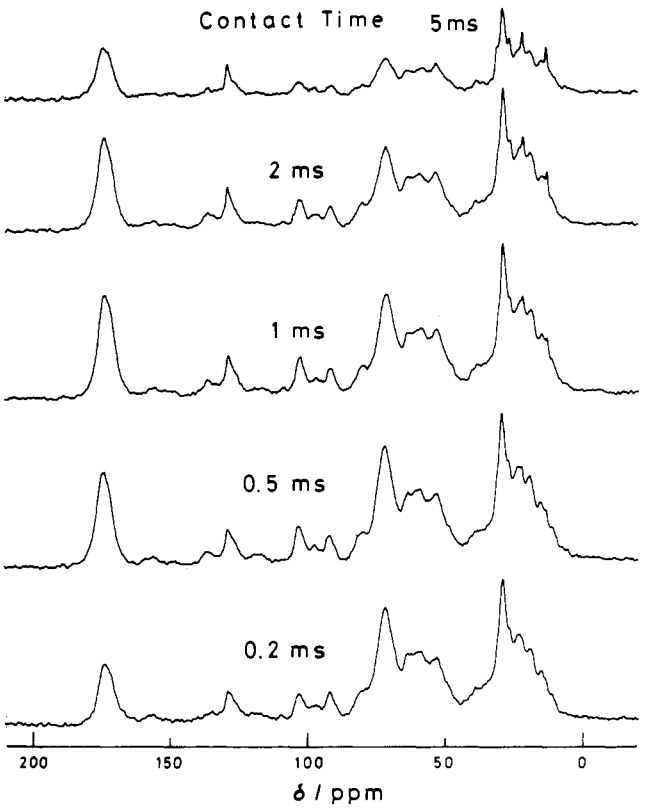

FIGURE 1: Cross-polarization magic-angle spinning (CP/MAS) carbon-13 NMR spectra of the freeze-dried intracytoplasmic membrane (ICM) of *Rhodopseudomonas palustris*. The spectra were recorded on a Bruker CXP-300 FT NMR spectrometer with the carbon-13 frequency of 75.46 MHz. The proton decoupling field was 1.17 mT. The sample consisted of ca. 150 mg of the material packed in an Andrew type rotor made of boron nitride. The spectra were obtained with Dixon's TOSS pulse program with variable contact times. The spectral bandwidth was 30 kHz with a 4-kW memory size. The spinning rate was 3330 Hz. The spectra were obtained from 2000 accumulations with a 5.0-s recycle delay, 20-ms observation time, and 30-Hz line broadening. Chemical shifts are reported to external Me_4Si. The peak heights were proportional to the absolute intensity.

mainly the resonances from the lipids. The characteristic features with varied contact times originate from the relaxation behavior which will be discussed later.

Solid-State ^{13}C NMR of LH2. The solid-state ^{13}C CP/MAS observation was also applied to the BChl–protein complex (LH2). A series of spectra of LH2 are shown in Figure 3. The spectra were taken with contact times from 100 μs to 5 ms. The gross features of these spectra change greatly with the contact time.

Assignments for each carbon in LH2 were made on the basis of known chemical shift values from spectra of model compounds in solutions (Wüthrich, 1976; Brereton & Sanders, 1983). The peaks in the region from 170 to 180 ppm are due to carbonyl carbons. The resonances in the range 120–140 ppm are assigned to aromatic and olefinic carbons. The band at ca. 72 ppm is mostly due to the methylene and methine carbons adjacent to an oxygen atom. The signals may have some contributions from the methylene carbons of Triton X-100. The shoulder that appears at 68 ppm is assigned to the C_β carbons of threonine residue. The resonances in the 45–65 ppm range are assigned to the C_α carbons of the peptide backbones. The peak around 37 ppm is due to the carbons of the BChl *a* phytol chain [P_n (n = 4, 6, 8, 10, 12, 14) in Figure 6]. The biggest peak at 31 ppm is attributable to the valine C_β, the proline C_β, the lysine C_δ, the glutamine C_γ, the methionine C_β and C_γ, and the phytyl methine carbons [P_n

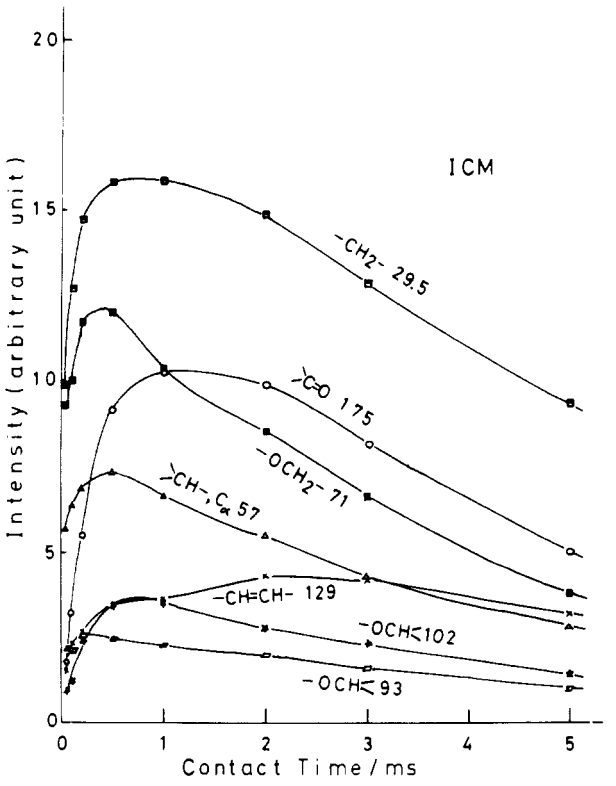

FIGURE 2: Cross-polarization magnetization (in relative intensity) vs. contact time plot for the freeze-dried ICM of *Rps. palustris* under the CP/MAS conditions. The types of carbon structures for the signals are given along with the chemical shifts as numerical values.

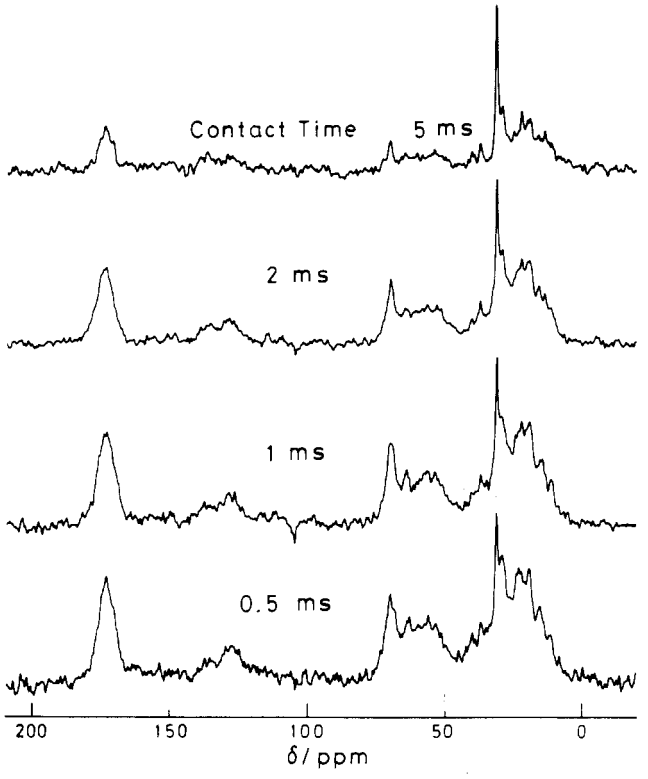

FIGURE 3: Stack plots of variable contact time spectra of the freeze-dried LH2 of *Rps. palustris* with Dixon's TOSS pulse program. The spectra were obtained from 33 000 to 20 000 scans with 50 mg of the sample. The other conditions are the same as those in Figure 1. The tallest peak in each spectrum was scaled to a uniform height.

(n = 7, 11, 15) in Figure 6]. The methylene carbons of the fatty acid of the lipid were also found to have peaks in this chemical shift region as mentioned below. The NMR peak around 29 ppm is due to the C_β carbons of lysine, arginine,

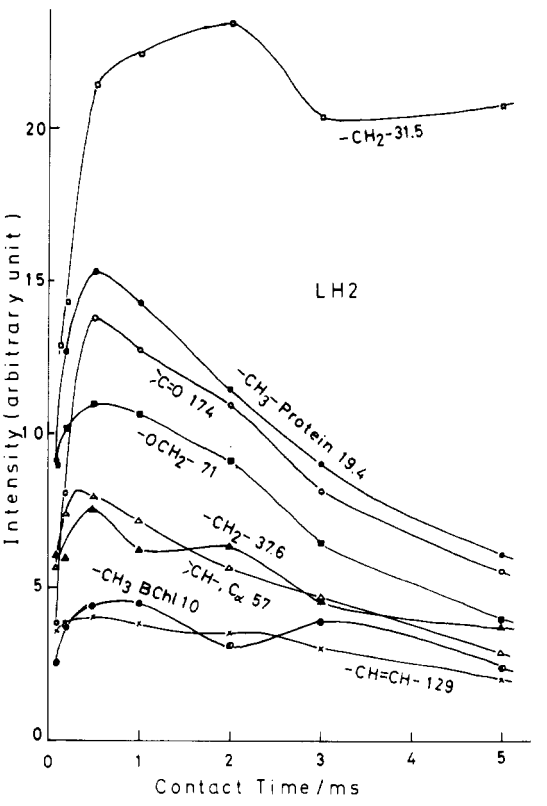

FIGURE 4: Cross-polarization magnetization (in relative intensity) vs. contact time plot for the freeze-dried LH2 of *Rps. palustris* under the CP/MAS conditions. The types of carbon structures for the signals are given along with the chemical shifts as numerical values.

glutamine, tryptophan, and histidine residues. The band around 23 ppm is assigned to the methyl carbon of leucine and the C_γ carbon of lysine residues. The peak at 22 ppm is due to the methylene carbons adjacent to the terminal methyl of the fatty acid. The peaks at 15 and 19 ppm are assigned to the methyl carbons of the peptide amino acid residues of alanine, valine, isoleucine, and methionine. The peaks and shoulder at 9, 10, and 12 ppm are due to the methyl carbons in the BChl ring. It should be mentioned that a small quantity of lipid exists in our LH2 preparation. This fact was confirmed also by solution-state ^{13}C NMR studies. Thus, the LH2 in D_2O showed the peak at 31.5 ppm which can be attributed to the fatty acid (the results which will be published separately). It is very interesting to determine whether these lipids are intrinsic ones or not in connection with the boundary lipids which strongly interact with the proteins (McLaughlin et al., 1981).

The relative signal intensities for each resolved resonances were plotted vs. the contact times (Figure 4). The contact time dependence of the signal intensity shows a steep increase up to 1 ms and a gradual decay after that time.

From the known amino acid analysis data (Hayashi et al., 1982c) and the chemical shift data (Wüthrich, 1976), the relative signal intensities at each chemical shift are plotted in Figure 5 as a bar graph. The observed ^{13}C NMR spectrum with the contact time of 0.5 ms is also overlaid in Figure 5. It is seen from this figure that the signals for the relatively short contact time come mainly from the resonances from the proteins.

In Figure 6 the ^{13}C NMR spectrum of LH2 with the long contact time (5 ms) is compared with that of BChl *a* in a solution, which is drawn from the chemical shift data of the solution BChl *a* spectrum (Brereton & Sanders, 1983). The magnitudes of the bars in Figure 6 were taken in proportion

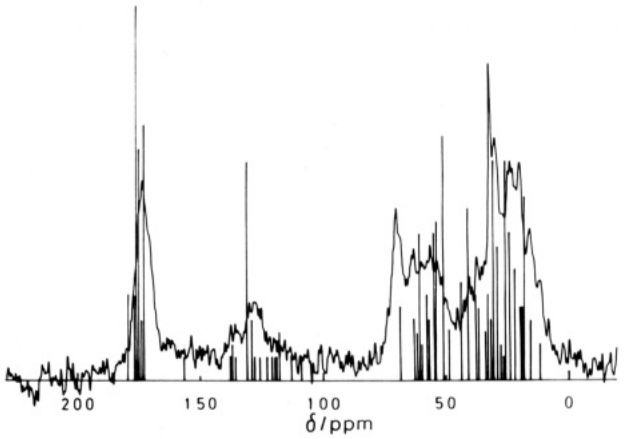

FIGURE 5: Comparison of the 0.5-ms contact time spectrum in Figure 3 with the simulation spectrum for the LH2 proteins. The simulation spectrum was obtained from the known amino acid analysis data of LH2 and the known chemical shift data (see text). The magnitudes were taken in proportion to the number of carbons.

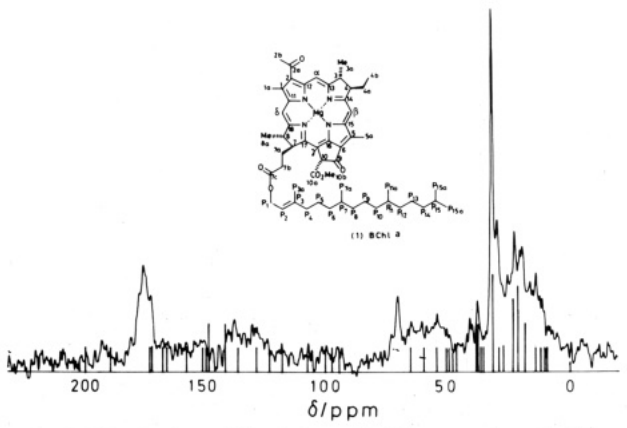

FIGURE 6: Comparison of the 5-ms contact time spectrum in Figure 3 with the simulation spectrum for BChl *a*. The simulation spectrum was obtained from the known chemical shift data for BChl *a* (see text). The magnitudes were taken in proportion to the number of carbons.

to the numbers of the carbons. It can be recognized that the ^{13}C NMR spectrum with the long contact time of 5 ms is similar to the resonances from BChl *a*. It also contains the ^{13}C NMR signals attributable to the lipids at 31.5 ppm.

DISCUSSION

Characteristics of a Cross-Polarization Experiment and Determination of NMR Parameters (T_{CH} and $T_{1\rho}^{H}$). In the cross-polarization pulse sequence (Lowe, 1959), the proton spins are "spin locked" by giving them a 90° pulse and then "locking" them in the x,y plane with a pulse duration which is phase shifted by 90° from the first pulse. When the proton spins are locked, the carbon spins are simultaneously subjected to a pulse, also of duration τ, fulfilling the Hartmann–Hahn condition. The effect of this matching of the spins is to produce an enhancement of the carbon magnetization which is detected at the end of the time period, τ, by turning off the carbon pulse and by recording the carbon free-induction decay, the proton pulse being kept on for a further time period as a dipolar decoupling field. After a time period, T, during which the proton magnetization recovers, the pulse sequence may be repeated.

Magnetization induced at the cross-polarization time (contact time) τ can be described as (Garroway et al., 1979; Mehring, 1983)

$$M(\tau) = M_0\lambda^{-1}[1 - \exp(-\lambda\tau/T_{CH})] \exp(-\tau/T_{1\rho}^{H}) \quad (1)$$

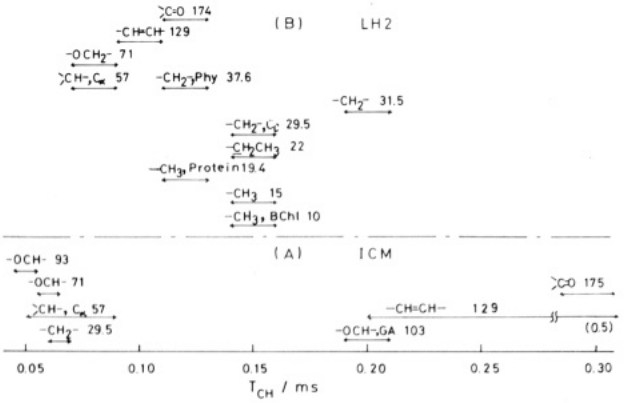

FIGURE 7: Range of T_{CH} values for the signals at the respective chemical shift of ICM (A) and LH2 (B) of *Rps. palustris*. The types of carbon structures for the signals are given along with the chemical shifts as numerical values.

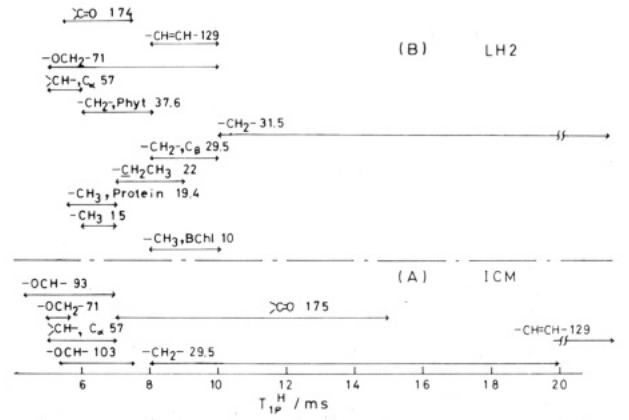

FIGURE 8: Range of $T_{1\rho}^{H}$ values for the signals at the respective chemical shift of ICM (A) and LH2 (B) of *Rps. palustris*. The types of carbon structures for the signals are given along with the chemical shifts as numerical values.

where $\tau = 1 + (T_{CH}/T_{1\rho}^{C}) - (T_{CH}/T_{1\rho}^{H})$, where $T_{1\rho}^{H}$ and $T_{1\rho}^{C}$ represent the spin–lattice relaxation times in the rotating frame for ^1H and ^{13}C, and where T_{CH} denotes the time constant for the cross-polarization under spin-lock conditions. The equilibrium carbon magnetization, M_0, is determined by the proton spin temperature. For large radio-frequency fields, $M_0 = (\gamma_H/\gamma_C)M_0^C$, where M_0^C is the ordinary carbon thermal magnetization appropriate for the static field. (Here, $T_{1\rho}^{C}$ in this expression, however, denotes that corresponding to $\omega_{1C} + \omega_{1H}$ radio frequency and not to ω_{1C} as usual.) Equation 1 admits a simple interpretation: the carbon magnetization rises with the rate T_{CH}^{-1} while being depleted at $(T_{1\rho}^{H})^{-1}$. Since a quantitative analysis of Figures 2 and 4 shows $T_{CH} \ll T_{1\rho}^{H}$, $T_{1\rho}^{C}$ in these systems, λ can be set to 1. Then eq 1 becomes

$$M(\tau) = M_0[1 - \exp(-\tau/T_{CH})] \exp(-\tau/T_{1\rho}^{H}) \quad (2)$$

From this equation T_{CH} and $T_{1\rho}^{H}$ can be evaluated by a simulation method from the observed results in Figures 2 and 4. The results are summarized in Figures 7 and 8.

The cross-polarization (CP) technique enhances the signal/noise ratio of the carbon-13 spectrum in two ways. First, there is a direct enhancement as the carbon magnetization is increased by the cross-polarization to a maximum of approximately 4 times (the ratio of the magnetogyric ratios). Second, the cross-polarization technique does not depend on the carbon-13 spin–lattice relaxation times, which may be long, but depends only on the proton spin–lattice relaxation times which are usually much shorter. The cross-polarization pulse sequence may, therefore, be repeated with a relatively short

time interval, T, chosen as that the proton magnetization has recovered, which yields an increase in the carbon signal intensities in a given time period. This second effect will be most important for signals due to carbon nuclei with longer relaxation times.

The cross-polarization pulse sequence gives very substantial gains in the intensity of the carbon-13 spectrum, but there are several points at which discrimination may occur within the carbon spins (Dudley & Fyfe, 1982). Typical examples are shown in Figures 5 and 6 where the ^{13}C NMR signals of the protein and BChl *a* were relatively selected, respectively. During the "contact" of the carbon and proton spins in the cross-polarization sequence, the magnetization of a particular carbon will increase with a cross-polarization time constant, T_{CH}, reach a maximum value, and decay with either the loss of proton magnetization described by $T_{1\rho}^{H}$ or by $T_{1\rho}^{C}$, or by some combination of these. The cross-polarization time constant T_{CH}^{i} for the ith carbon depends on the proton–dipolar interactions to that carbon which in turn are related to the sixth power of the C^{i}–H internuclear distances (Demco et al., 1975). In general, a distribution of T_{CH}^{i} values may be expected, a particularly large difference predictably occurring between carbons with no attached hydrogen and those which have one or more attached hydrogens. Thus, the increase in the carbon magnetizations may differentiate binding modes of carbons. Further, during the contact time, the proton magnetization will decay according to $T_{1\rho}^{H}$ which may differentiate dynamic modes of carbons.

Estimation of Correlation Times. The $T_{1\rho}^{H}$ values have a dependency on an applied radio frequency expressed as (Douglass & Jones, 1966)

$$1/T_{1\rho}^{H} = H_d^2[\tau_c/(1 + 4\omega_1^2\tau_c^2)] \quad (3)$$

when dipole–dipole interactions are predominant in relaxation mechanisms. In eq 3 H_d denotes the decoupling field strength, and τ_c expresses the correlation time of the molecular motion. The $T_{1\rho}^{H}$ value gives a minimum at the correlation time τ_c of $1/\omega_{1H}$. In these experiments ω_{1H} was set to be 11.7×10^{-4} T which means 5×10^4 Hz. Hence, $1/\omega_{1H}$ is equal to 2×10^{-5} s. Since, in the biological system as treated here, the molecular weight of the component molecules is very large, the molecular motions that affect $T_{1\rho}^{H}$ values will be local segmental motions rather than total molecular rotations. The order of the local motions of the polypeptide backbones is expected to be shorter than 2×10^{-5} s (Jardestzky & Roberts, 1981). Hence, the correlation times for these molecular motions can be taken to be shorter than that for the $T_{1\rho}^{H}$ minimum. Therefore, in the system treated here we can discuss the local molecular motion from the $T_{1\rho}^{H}$ values as described below.

Dynamic Structures of ICM and LH2. The $T_{1\rho}^{H}$ value is correlated not only with motional behavior but also with the effects of spin diffusion and paramagnetism (Douglass & Jones, 1966; VanderHart & Garroway, 1979; McBrierty et al., 1972). A comparison of parts A and B of Figure 8 demonstrates that ICM has similar orders of $T_{1\rho}^{H}$ values as compared with those of LH2 which contains no paramagnetic center. This means that the paramagnetic effect is also minor in ICM. Since the spin diffusion mechanism works especially in a crystalline system (a hard solid), this mechanism cannot be predominant for the ICM system which is amorphous (not crystalline). Therefore, we can compare the motional behavior of ICM with that of LH2 from $T_{1\rho}^{H}$ values.

T_{CH} values of carbon atoms depend on the numbers of protons (the directly attached protons and/or neighboring protons) which interact with the particular carbons. T_{CH} values are also correlated with motional behavior. The faster molecular motion decreases the efficiency of the cross-polarization, thus making the T_{CH} value long.

The large portion of the dry weight of the isolated ICM is composed of proteins and lipids. Up to 8% of their dry weight is made of photosynthetic pigments (Niederman & Gibson, 1978).

The carbon signals of the lipids are composed of ^{13}C resonances from the fatty acids, the glycerol backbones, and the polar head groups. In ICM the carbonyl carbons, the unsaturated carbons, and the methylene carbons of the fatty acids, which display signals around 175, 129, and 29.5 ppm, have $T_{1\rho}^{H}$ values of 7–15, 20, and 8–20 ms, respectively, while the carbons of the glycerol backbone and the glycerol polar head group give the signal at 71 ppm and have a $T_{1\rho}^{H}$ value of 5 ms. Since the $T_{1\rho}^{H}$ values in these systems are correlated especially with the local molecular motions as discussed before, these $T_{1\rho}^{H}$ values indicate the higher mobility of the fatty acid chains than those of the glycerol backbones and the polar head groups. A similar situation was found from the observed T_{CH} values. Figure 7B shows that the carbonyl carbons, the olefinic carbons, and the glycerol carbons have T_{CH} values of 0.30, 0.2–0.5, and 0.06–0.07 ms, respectively. These T_{CH} values suggest faster local motions of the carbonyl and olefinic carbons (which have the longer T_{CH} values) than that of the glycerol carbons (which have the shorter T_{CH} values). The relatively longer T_{CH} values for the carbonyl carbons are also due to the lack of directly bound protons.

The motional behavior of the peptide backbones can be explored from 50–65 ppm signals, since there are essentially no contributions to these signals from other chemical structures. The C_α carbons yielded the T_{CH} values of 0.05–0.09 ms and the $T_{1\rho}^{H}$ values of 5–7 ms for ICM, while they gave the T_{CH} values of 0.07–0.09 ms and the $T_{1\rho}^{H}$ values of 5–6 ms for LH2. These observations indicate that the polypeptide backbones have similar local molecular motions in both ICM and LH2. However, a little bit wider range of these T_{CH} and $T_{1\rho}^{H}$ values for ICM is noticeable, indicating a greater range of motional freedom for the peptide backbones in ICM than those in LH2.

In ICM the carbonyl carbons showed the $T_{1\rho}^{H}$ values of 7–15 ms, while those in LH2 showed the $T_{1\rho}^{H}$ values of 5.5–7.5 ms. The signals in LH2 mainly come from those of peptide backbones because of the essential lack of lipids, while the signals in ICM have contributions from those of the peptide backbones and the lipid backbones. Since the carbonyl carbons of the peptide backbones should have similar local motions to those of peptide C_α carbons, they should have similar orders of $T_{1\rho}^{H}$ values both in ICM and in LH2. Therefore, the longer part of $T_{1\rho}^{H}$ in ICM carbonyl carbons can be attributed to the carbonyl carbons of the fatty acid esters. Thus, the faster local molecular motions were revealed for the lipid fatty acid in ICM as compared with the peptide backbones.

The ^{13}C NMR signals in the aromatic region showed the T_{CH} values of 0.2–0.5 ms and the $T_{1\rho}^{H}$ values of 10–20 ms for ICM and the T_{CH} values of 0.09–0.11 ms and the $T_{1\rho}^{H}$ values of 8–10 ms for LH2. The observed signals are mostly due to the aromatic carbons from amino acid residues and BChl *a* in LH2. The longer components of T_{CH} and $T_{1\rho}^{H}$ in ICM may be attributed to the ^{13}C NMR signals from the olefinic carbons of the fatty acid chains in the lipids.

For LH2 the signal at 31.5 ppm has the $T_{1\rho}^{H}$ value longer than 20 ms, for which a very fast molecular motion is predicted. This is most probably explained by the contribution from the remaining lipid. The longer component at the

ethylene oxide signal may be attributable to the Triton X-100 contamination.

The resolved ^{13}C NMR peaks which can be assigned to BChl *a* are only those for the methyl carbon at 10 ppm and the phytyl methine carbons at 37.5 ppm. The olefinic carbons and the carbonyl carbons for BChl *a* are not resolved under large signals from proteins and lipids. The $T_{1\rho}^{H}$ value of the methyl group of BChl *a* was 8–10 ms, and those of the methine carbons of the phytyl residues were 6–8 ms. These values show the faster molecular motion for the BChl methyl carbon than for the phytyl methine carbons. The slow local molecular motions of the BChl phytyl methine carbons should be compared with the faster ones of the lipid fatty acid methylene. *This indicates that the phytol chain is buried in the protein rather than in the lipid fatty acid.* The T_{CH} values of the BChl methyl carbon (0.14–0.13) and the phytyl methine carbons (0.11–0.13) also suggest the faster local molecular motion for the BChl methyl carbon than for the phytyl methine carbons.

For LH2 $T_{1\rho}^{H}$ and T_{CH} values for the methylene carbons of the protein are longer than those for the methyl carbons of the protein. These facts indicate faster local motions for the methylene type carbons than the methyl ones in the protein.

In conclusion it was exemplified that the ^{13}C NMR spectra of the selective components (lipid, protein, or BChl *a*) in a complex biological system (a photosynthetic membrane) can be obtained by a suitable selection of the contact time. Shorter contact times (0.5–1 ms) favored the ^{13}C NMR signals attributable to the protein parts for both ICM and LH2. The ^{13}C resonances of lipid or BChl *a* emerged in the observations with relatively longer contact times (ca. 5 ms).

The values of the relaxation time $T_{1\rho}^{H}$ and the cross-polarization time constant T_{CH} indicate (1) the faster local molecular motion of the lipid fatty acid as compared with the glycerol backbone and the polar head group, (2) the essentially similar molecular motions of the protein backbones both in ICM and in LH2 (less fundamental roles of the lipid for these molecular motions), and (3) the presence of the BChl phytyl chain in the protein but not in the lipid.

ACKNOWLEDGMENTS

We express our heartfelt thanks to Professor Shigehiro Morita (Tokyo University of Agriculture and Technology) for his earnest encouragement throughout this study.

Registry No. BChl, 17499-98-8.

REFERENCES

Andrew, E. R. (1971) *Prog. Nucl. Magn. Reson. Spectrosc. 8*, 1–55.

Bremser, W., Ernst, L., & Franke, B. (1978) in *Carbon-13 NMR Spectral Data*, Verlag Chemie, Meinheim.

Brereton, R. G., & Sanders, J. K. M. (1983) *J. Chem. Soc., Perkin Trans. 1*, 435–437.

Brown, C. E., Spencer, R. B., Burger, V. T., & Katz, J. J. (1984) *Proc. Natl. Acad. Sci. U.S.A. 81*, 641–644.

Cohen-Bazire, G., & Sistrom, W. R. (1966) in *The Chlorophylls* (Vernon, L. P., & Seeley, G. R., Eds.) pp 313–341, Academic Press, New York.

Demco, D. E., Tegenfeldt, J., & Waugh, J. S. (1975) *Phys. Rev.* [*Sect.*] *B 11*, 4733–4738.

Dixon, W. T. (1982) *J. Chem. Phys. 77*, 1800–1809.

Douglass, D. C., & Jones, G. P. (1966) *J. Chem. Phys. 45*, 956–963.

Dudley, R. L., & Fyfe, C. A. (1982) *Fuel 61*, 651–657.

Garroway, A. N., Moniz, W. B., & Resing, H. A. (1979) *ACS Symp. Ser. No. 103*, 67–87.

Hayashi, H., Miyao, M., & Morita, S. (1982a) *J. Biochem.* (*Tokyo*) *91*, 1017–1027.

Hayashi, H., Nozawa, T., Hatano, M., & Morita, S. (1982b) *J. Biochem.* (*Tokyo*) *91*, 1029–1038.

Hayashi, H., Nakano, M., & Morita, S. (1982c) *J. Biochem.* (*Tokyo*) *92*, 1805–1811.

Jardestzky, O., & Roberts, G. C. K. (1981) in *NMR in Molecular Biology*, Academic Press, New York.

Lowe, I. J. (1959) *Phys. Rev. Lett. 2*, 285–289.

McBrierty, V. J., Douglass, D. C., & Falcone, D. R. (1972) *J. Chem. Soc., Faraday Trans. 2*, 1051–1059.

McLaughlin, A. C., Herbette, L., Blasie, J. K., Wang, C. T., Hymel, L., & Fleischer, S. (1981) *Biochim. Biophys. Acta 643*, 1–12.

Mehring, M. (1983) in *Principles of High Resolution NMR in Solids*, Chapter 4, pp 129–185, Springer, Berlin.

Niederman, R. A., & Gibson, K. D. (1978) in *The Photosynthetic Bacteria* (Clayton, R. K., & Sistrom, W. R., Eds.) pp 78–118, Plenum Press, New York.

Ohtsuka, Y., Nozawa, T., Tomita, Y., Tamai, Y., & Hatano, M. (1984) *Fuel 63*, 1363–1366.

Okazaki, M., & McDowell, C. A. (1984) *J. Am. Chem. Soc. 106*, 3185–3190.

Pines, A., Gibby, M. G., & Waugh, J. S. (1973) *J. Chem. Phys. 59*, 569–590.

Schaefer, J., & Stejskal, E. O. (1976) *J. Am. Chem. Soc. 98*, 1031–1032.

Sistrom, W. R. (1964) *Biochim. Biophys. Acta 283*, 492–504.

VanderHart, D. L., & Garroway, A. N. (1979) *J. Chem. Phys. 71*, 2773–2787.

Wüthrich, K. (1976) in *NMR in Biological Research: Peptides and Proteins*, Elsevier/North-Holland, New York.